

Saturated Liquid Densities and Vapor Pressures of Tetramethyl Orthosilicate Measured Using a Constant Volume Apparatus

Ann M. Anderson,^{*,†} Timothy B. Roth,[†] Matthew R. Ernst,[†] and Mary K. Carroll[‡]

Department of Mechanical Engineering and Department of Chemistry, Union College, Schenectady, New York 12308

This paper describes a simple constant volume technique that was developed to measure saturated pressure and saturated liquid density of tetramethyl orthosilicate (TMOS). The technique is based on the measurement of temperature and pressure of a liquid undergoing a constant volume heating process. We have observed that during such a process the pressure increases gradually as temperature is increased until the system reaches a “take-off” point where a rapid pressure rise occurs. Experimenting with methanol and water, we determined that the initial pressure/temperature data (pre take-off) can be used to estimate saturation pressure. We further determined that the take-off point occurs when the liquid expands to fill the container volume, which allows for calculation of the saturated liquid density. Using this information, we estimated and report on the saturated pressure and saturated liquid density of TMOS for temperatures from (60 to 250) °C.

Introduction

Tetramethyl orthosilicate (TMOS, $C_4H_{12}O_4Si$) is a clear, colorless liquid under room temperature and pressure. Its melting point is -2 °C and boiling point is (121 to 122) °C under atmospheric pressure. TMOS is used extensively as a precursor in the preparation of silica sol-gel films, monoliths, and powders. Hydrolysis of TMOS, in the presence of either an acid or base catalyst, followed by polycondensation reactions results in a porous gel with overall formula SiO_2 . The pores of the wet sol-gel are filled with methanol and water, which are byproducts of the hydrolysis and condensation reactions. TMOS can also be used in concert with other silica alkoxide precursors to make sol-gels with different overall chemical composition.

There is only a limited amount of property data for TMOS available in the literature. Kato and Tanaka¹ used an ebulliometer to measure liquid–vapor equilibria for binary systems of TMOS and tetraethoxide silane (TEOS). They present vapor pressure data for TMOS over the range of temperatures from (364 to 393) K. Ivannikov et al.² present TMOS liquid density and thermal conductivity data for temperatures between (283 and 323) K. Their density measurements were performed using a pycnometer. An extensive search of the literature yielded no other TMOS property data.

Our interest in the properties of TMOS stems from its use in the preparation of silica aerogels. Aerogels can be fabricated from wet sol-gels using ambient or supercritical drying techniques. The rapid supercritical extraction (RSCE) technique developed by Gauthier et al.³ uses high temperatures (up to 280 °C) to effect the supercritical drying of wet sol-gels that have pores filled with a methanol/water mixture. To better understand the RSCE process, it was necessary to determine the properties of TMOS at higher temperatures than those available in the literature.

In this paper, we describe a constant volume method for the determination of vapor pressure and saturated liquid density.

The technique is used to measure properties of TMOS for temperatures between (60 and 250) °C. The following section describes the technique and applicable theory. This is followed by sections describing verification experiments and TMOS results.

Constant Volume Technique

The constant volume property estimation technique relies on measurements of the pressure–temperature relationship that occurs during heating in a constant volume process. Consider water heated in a sealed, constant-volume container. Unless the container is completely filled with water, it will also contain some air. As the water is heated, it will expand and the air will compress (and some will dissolve in the liquid water). The pressure in the container is made up of the partial pressure of the constituents: water and the components making up the air mixture. The water will exist in both liquid and vapor form during this process. Therefore, the partial pressure of the water will be its saturation pressure at the given temperature. We can use measurement of the container pressure to estimate the saturation pressure of a substance as a function of temperature.

At some temperature the water expands to fill the volume of the container (that which is not occupied by air). Upon further heating, the pressure rises rapidly, and the process becomes a constant specific volume process. Given the initial mass of the water and the container volume, we can calculate the saturated liquid density (assuming the container is pressure resistant to deformation at the conditions of the measurement and the volume of compressed air is negligible). The temperature at which this value applies is determined from the pressure–temperature relation. By varying the initial volume of water in the container and observing the pressure–temperature relation, we can establish the saturated liquid density as a function of temperature.

A pressure–temperature plot for the constant-volume heating of methanol is shown in Figure 1. Initial volumes of methanol from (3.00 to 5.00) mL were heated in a 5.55 mL sealed container. For each initial volume of methanol, the pressure closely follows the vaporization line for methanol (indicating

* Corresponding author. E-mail: andersoa@union.edu. Phone: 518-388-6537. Fax: 518-388-6789.

[†] Department of Mechanical Engineering.

[‡] Department of Chemistry.

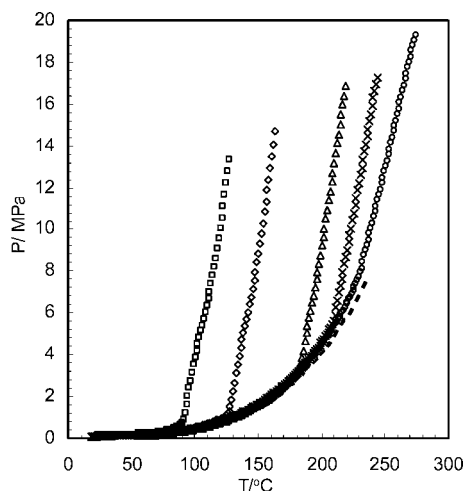


Figure 1. Typical pressure/temperature curves for methanol heated in a constant-volume process with a range of initial fill volumes from (3.0 to 5.0) mL. □, 5.0 mL; ◇, 4.6 mL; △, 4.0 mL; ×, 3.6 mL; ○, 3.0 mL; - - vaporization line (from ref 4).

that the partial pressure of the air is small) until it reaches a “take-off” point where a large pressure increase is observed. The take-off temperature increases as the initial volume of liquid decreases. In each case, the take-off point indicates the location at which the initial volume of methanol has expanded to fill the container.

Estimation of Saturated Liquid Density. We assume that the liquid initially placed in the container has expanded to fill the container when the large pressure rise (i.e., a rapid rate of change of pressure with temperature) occurs (the take-off point). At this point, we can calculate the saturated liquid density, ρ_f as

$$\rho_f = \frac{m_{\text{liq}}}{V_c} \quad (1)$$

where m_{liq} is the mass of the liquid originally placed into the container and V_c is the volume of the container. Through identification of the take-off point (as described in the Saturation Density Estimates of Water and Methanol section, below) on the pressure–temperature curves under constant volume heating conditions, we can find the saturated liquid density as a function of temperature. By varying the amount of liquid initially placed in the container, we can measure densities over a range of temperatures.

Estimation of Saturation Pressure. The pressure measured during this heating process represents the total pressure of the liquid/air mixture, P_T . To calculate the saturation pressure in the pre take-off region, P_{liq} , at each temperature, T , we use Dalton’s Law and correct the measured pressure by subtracting off the partial pressure of the air, P_{air} , in the container

$$P_{\text{liq}} = P_T - P_{\text{air}} \quad (2)$$

We can estimate the pressure of the air using the ideal gas law

$$P_{\text{air}} = \frac{n_{\text{air}}RT}{V_{\text{air}}(T)} \quad (3)$$

where R is the universal gas constant; T is the temperature; n_{air} is the number of moles of air in the container, and $V_{\text{air}}(T)$ is the volume occupied by the air at the specified temperature.

The number of moles of air is constant and is estimated from initial conditions. The volume of air at any time during the

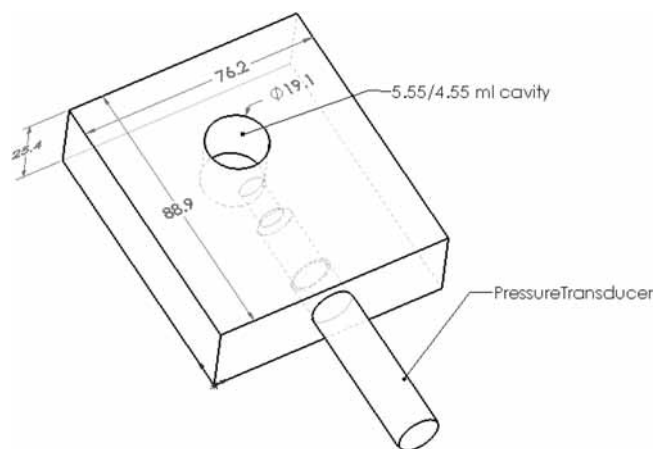


Figure 2. Schematic of the mold/cell apparatus used for measuring the temperature and pressure during heating. All dimensions are in millimeters.

process is estimated as the difference between the container volume (fixed) and the liquid volume which changes with temperature

$$V_{\text{air}}(T) = V_c - \rho_f(T) * m_{\text{liq}} \quad (4)$$

The saturated liquid density is calculated using an estimate of saturated liquid density as a function of temperature as described in the Estimation of Saturated Liquid Density section. At each temperature in the applicable range, the saturated liquid density is calculated, multiplied by the initial mass of liquid in the container, and subtracted from the container volume to get the air volume. This air volume value is then substituted into eq 3, from which the air pressure is calculated and then subtracted from the measured pressure to get the saturation pressure in eq 2. These equations are only applicable in the pre take-off region, where we assume a nonzero air volume.

The following sections describe a set of experiments performed using substances whose properties are well documented. The results are used to verify the constant volume property estimation technique.

Methods And Materials

Materials. Tetramethylorthosilicate (TMOS, CAS 681-84-5) was purchased from Sigma-Aldrich at 99+ % purity. Reagent-grade methanol, acquired from Fisher Scientific, and laboratory quality deionized water were used without further treatment.

Apparatus. The method employed here utilized measurements of temperature and pressure during a constant-volume heating process. The apparatus consists of a single-cell steel mold and a method for heating and sealing that mold. As seen in Figure 2, the mold is (88.9 by 76.2 by 25.4) mm high. The cell has a diameter of 19.1 mm and is 19.1 mm deep. The mold was instrumented with a melt pressure temperature transducer, which measured both temperature and pressure (Transducer Direct, 0-10-V, 68.9 MPa range with an accuracy of 0.5 % of full scale). This type of transducer uses a strain gauge to measure the deflection of the diaphragm and determine pressure and a thermocouple to measure temperature. They are widely used in injection molding applications and can operate under high temperature and pressure conditions. The empty volume of the cell is (5.55 ± 0.05) mL which was estimated by measuring the amount of liquid required to fill it. This value is larger than that calculated using the cell dimensions due to a small cutaway for the pressure transducer. To evaluate the effect of cell volume

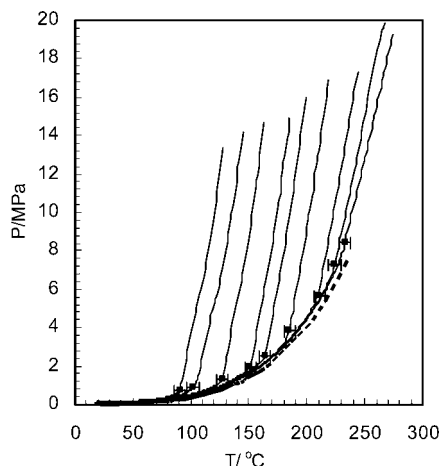


Figure 3. Pressure/temperature curves for methanol in a 5.55 mL mold for initial volumes from (3.0 to 5.0) mL. From left to right, the lines represent results for initial fill volumes of (5.0, 4.8, 4.6, 4.4, 4.2, 4.0, 3.6, 3.3, and 3.0) mL. The take-off points are identified by black squares. The dotted line is the vaporization line for methanol (ref 4). The error bars represent the scatter in repeated measurements (± 5 °C).

on the constant volume property estimation technique, we also used a mold with volume (4.55 ± 0.05) mL.

In a typical experiment, a specified volume of liquid was measured using an Eppendorf maxipettor and poured into the mold. We used a 0.0254 mm piece of Kapton film (American Durafilm) and a 1.59 mm thick piece of graphite (Phelps Industrial Products) to seal the mold. The entire assembly was then placed between the platens of a hydraulic hot press, which provided a clamping force of 140 kN and sealed the mold. The 140 kN setting was capable of sealing the mold up to internal pressures of 17.2 MPa. The hot press also provided a method for heating the mold. Alternatively, the mold could be sealed using bolts and heated using a high temperature film heater. We heated the mold as fast as the hot press allowed (a rate of 7.5 °C \cdot min $^{-1}$). Tests at slower rates yielded the same temperature/pressure results, indicating that equilibrium thermodynamics applies. The pressure and temperature measured by the transducer were recorded every 8 s during the heating process.

Uncertainty Estimates. An uncertainty estimate for each variable was determined through repeatability tests or from the manufacturer specifications. The temperature, which was measured by a type J thermocouple, has an uncertainty of 1 °C. The experimental take-off point temperature, under constant conditions, was found to be repeatable within a maximum deviation of ± 5 °C. The uncertainty in the cell pressure is quoted as ± 0.3 MPa or 0.5 % of the full scale. A calibration showed the uncertainty to be ± 0.05 MPa at pressures below 5.5 MPa. The volume of liquid was repeatable within a maximum deviation of ± 0.05 mL.

Verification of the Constant Volume Technique

Saturation Density Estimates of Water and Methanol.

Figures 3 and 4 plot the pressure–temperature (PT) curves for pure methanol and pure water. The initial volume was varied from (3.50 to 5.00) mL (water) and (3.00 to 5.00) mL (methanol). As described above, the pressure rises gradually as temperature is increased until the take-off point is reached and the pressure starts to rise rapidly. To determine the take-off temperature, we examined the PT plots and located the point at which the pressure started to increase more rapidly with temperature. Since the determination of this point can be difficult, we defined it as the location where the pressure

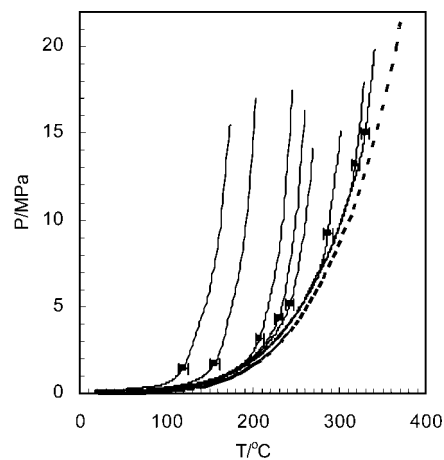


Figure 4. Pressure/temperature curves for water in a 5.55 mL mold for initial volumes from (3.5 to 5.0) mL. From left to right, the lines represent results for initial fill volumes of (5.0, 4.8, 4.5, 4.4, 4.3, 4.0, 3.6, and 3.5) mL. The take-off points are identified by black squares. The dotted line is the vaporization line for water (ref 4). The error bars represent the scatter in repeated measurements (± 5 °C).

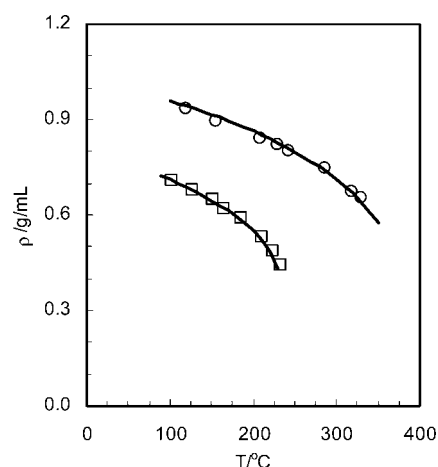


Figure 5. Saturation liquid densities for water and methanol estimated by the constant volume technique superimposed on data from the NIST database. Error bars are left out for clarity but are approximately the same size as the symbols. \square , methanol; \circ , water; —, from ref 4.

deviated from the pressure measured at the same temperature for the smallest fill volume data by more than 5 % of the critical pressure value (a difference of 1 MPa for water and 0.4 MPa for methanol). The smallest fill volume data (3.00 mL for methanol and 3.50 mL for water) was used as a reference because it has the highest take-off temperature. To estimate the take-off temperature for the 3.00/3.50 mL fill volumes, we extrapolated the pre take-off PT curve to determine the take-off point. The estimated take-off points are indicated as black squares in the PT plots of Figures 3 and 4. Both water and methanol tests were performed in the 5.55 mL cell.

Using eq 1, we calculated the saturated liquid density for each initial volume. The experimental uncertainty of the measured density is estimated to be less than 3 %. This value takes into account the uncertainty in the mold volume (± 0.05 mL) and the uncertainty in the initial volume of liquid (± 0.05 mL).

Figure 5 plots the calculated saturated liquid density for water and methanol versus take-off temperature and compares these values to data obtained from a NIST database (Lemmon et al.⁴). The density estimates for both water and methanol show strong agreement with the database: nearly all values estimated from our data overlap the database line within error bars.

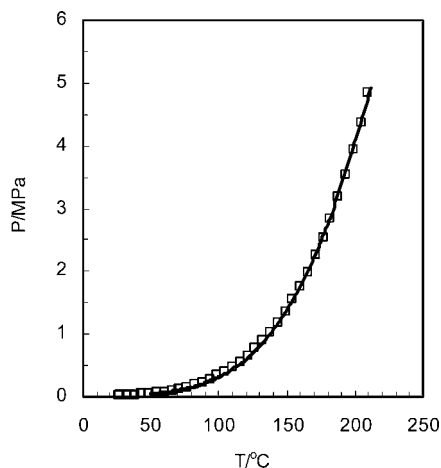


Figure 6. Plot of the methanol saturation pressure estimated from the 3 mL volume data (solid line) and saturation pressure data for methanol from the NIST database (ref 4, open squares). Note that standard values overlap the estimation line throughout the temperature region measured.

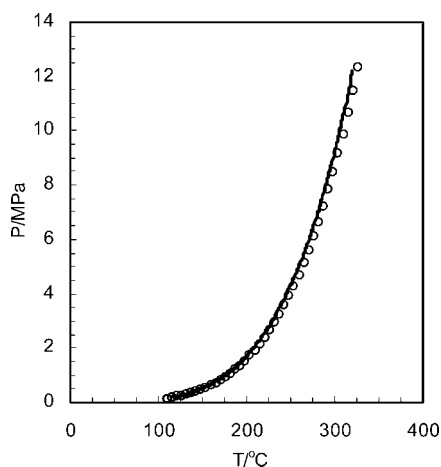


Figure 7. Plot of the water saturation pressure estimated from the 3.5 mL volume data as a function of temperature (solid line) and water saturation data from the NIST database (ref 4, open circles). The saturation estimation overlaps with standard data from (120 to 190) °C but appears to give systematically higher results at temperatures above 190 °C.

Saturation Pressure Estimate of Water and Methanol. We calculated the saturation pressure as a function of temperature using the procedure described in the Estimation of Saturation Pressure section. In each case, we used pressure data from the test with 3.00 mL (methanol) or 3.50 mL (water) of liquid in the 5.55 mL mold. The small volume provides the longest range of data (i.e., the takeoff point does not occur until 230 °C for methanol and 330 °C for water). The results of this calculation are shown in Figures 6 and 7 for methanol and water. The data are compared to data from NIST (Lemmon, et al.⁴). The estimated saturation pressure of methanol overlaps with the NIST data over the entire temperature range [(50 to 210) °C]. The estimated saturation pressure for water overlaps with NIST data for temperatures between (120 and 190) °C but yields systematically higher results above 190 °C.

Estimation of TMOS Properties

TMOS was tested in two different molds. Figure 8 shows the pressure and temperature measurements for the 4.55 mL mold, whereas Figure 9 shows the results for the 5.55 mL mold. Both plots show data for a range of initial liquid volumes. We defined the take-off point as the location where the pressure

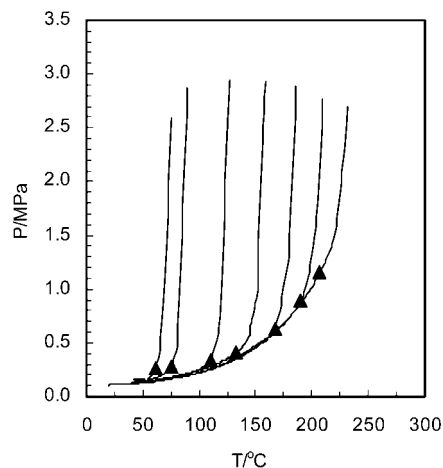


Figure 8. Pressure/temperature curves for TMOS in a 4.55 mL mold for initial liquid TMOS volumes from (3.0 to 4.2) mL. From left to right, the lines represent results for initial fill volumes of (4.2, 4.0, 3.8, 3.6, 3.4, 3.2, and 3.0) mL. The take-off points are identified by black triangles.

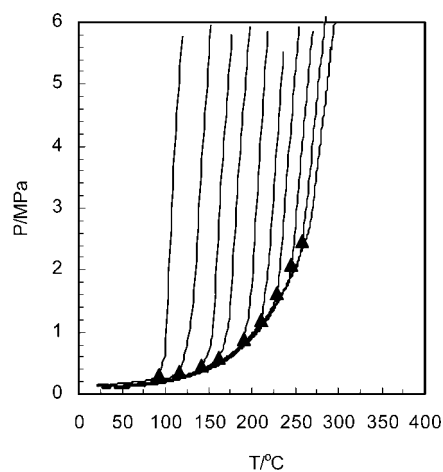


Figure 9. Pressure/temperature curves for TMOS in a 5.55 mL mold for initial liquid TMOS volumes from (3.0 to 4.8) mL. From left to right, the lines represent results for initial fill volumes of (4.8, 4.6, 4.4, 4.2, 4.0, 3.8, 3.6, 3.4, 3.2, and 3.0) mL. The take-off points are identified by black triangles.

deviated from the PT curve by more than 5 % of the critical pressure value (a difference of 0.1 MPa for TMOS). The take-off points are indicated by the solid symbols in the plots.

Figure 10 is a plot of the saturated liquid density for TMOS calculated from eq 1 versus temperature. The values measured in the 4.55 mL mold are indistinguishable from those measured in the 5.55 mL mold. The figure also gives a plot of TMOS data from Kato and Tanaka¹ (room temperature) and Ivannikov et al.² Although the existing data is for temperatures lower than those measured in this study, our results are consistent with these data. Saturated liquid density values for TMOS are included in Table 1.

A third-order polynomial fit to the data gives the following empirical relation between the saturated liquid density of TMOS and temperature

$$\rho_f = -2.26 \cdot 10^{-8} T^3 + -9.88 \cdot 10^{-6} T^2 - 3.05 \cdot 10^{-3} T + 1.14 \quad (5)$$

where the saturated liquid density is in units of $\text{g} \cdot \text{mL}^{-1}$ and temperature is in °C. This relation is valid only for the range of temperatures tested [(60 to 250) °C]. The best fit to the data

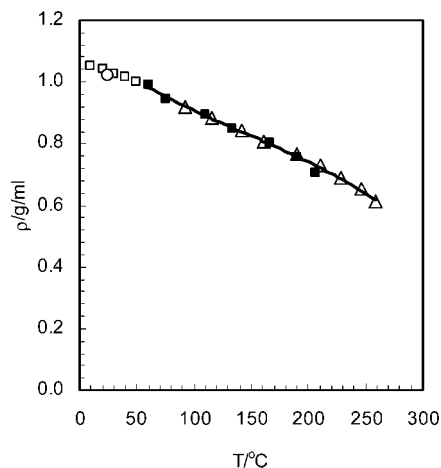


Figure 10. Estimated saturation liquid densities for TMOS based on measurements made using two molds with different volumes are in agreement. ■, 4.55-mL mold; △, 5.55 mL mold; □, Ivannikov et al. (ref 2); ○, Kato and Tanaka (ref 1). The solid line represents the fit to the estimated data given by eq 5.

Table 1. Saturated Liquid Density Values for TMOS Estimated by the Constant Volume Technique^a

temperature (°C)	density g·mL ⁻¹	
61	0.99	**
75	0.94	**
92	0.92	
110	0.90	**
116	0.88	
133	0.85	**
142	0.84	
161	0.80	
167	0.80	**
190	0.77	
190	0.75	**
207	0.71	**
210	0.73	
229	0.69	
246	0.65	
259	0.61	

^a Starred values were measured in the 4.55 mL mold. All other values were measured in the 5.55 mL mold.

proved to be a third-order polynomial with an *R*-squared value of 0.995. The polynomial model was chosen for ease of use.

Figure 11 is a plot of the estimate of TMOS saturation pressure vs temperature as calculated using eq 3 with the empirical relation for saturated liquid density (eq 5) for a 3.00 mL initial volume of TMOS in the 5.55 mL container. The only published TMOS data (Kato and Tanaka)¹ are also shown on the plot. Our TMOS saturation pressure data overlap consistently the higher end of the range of the Kato data. Saturated pressure data are included in Table 2.

The saturation pressure data were correlated using the Antoine equation with pressure in mm·Hg⁻¹ and temperature in K

$$\log P = A - \frac{B}{T + C} \quad (6)$$

The best fit to the Antoine equation yielded a $\Delta P/P_{\text{avg}} = 0.051$ for values of $A = 6.79$, $B = 1263$, and $C = -65.3$.

The uncertainty estimate for the TMOS saturation pressure data is shown in Figure 12. The estimate includes the measurement uncertainty in pressure, the uncertainty in the estimate of the TMOS density, and the uncertainty in the estimate of

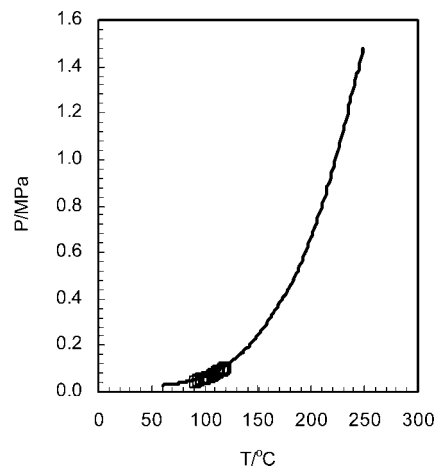


Figure 11. TMOS saturation pressure (solid line) estimated from the 3.0 mL volume data is shown to agree well with the Kato and Tanaka data (ref 1, open squares), which was taken over a limited range of temperatures.

Table 2. Saturated Pressure Values for TMOS Estimated Using Dalton's Law Applied to the 3.0 mL Volume Data

<i>T</i> °C	<i>P</i> MPa	<i>T</i> °C	<i>P</i> MPa	<i>T</i> °C	<i>P</i> MPa	<i>T</i> °C	<i>P</i> MPa
61	0.03	111	0.09	160	0.31	207	0.76
62	0.03	112	0.09	161	0.32	208	0.78
63	0.03	113	0.09	162	0.32	209	0.79
64	0.03	114	0.10	163	0.33	210	0.81
65	0.03	115	0.10	164	0.34	212	0.82
66	0.03	117	0.10	166	0.35	213	0.84
68	0.03	118	0.11	167	0.36	214	0.86
69	0.03	119	0.11	168	0.36	215	0.87
70	0.03	120	0.11	169	0.37	216	0.89
71	0.03	121	0.12	170	0.38	217	0.91
72	0.04	122	0.12	171	0.39	218	0.92
74	0.04	124	0.13	172	0.40	219	0.94
75	0.04	125	0.13	174	0.41	220	0.96
76	0.04	126	0.13	175	0.41	221	0.98
78	0.04	127	0.14	176	0.42	222	1.00
79	0.04	128	0.14	177	0.43	224	1.01
80	0.04	130	0.15	178	0.44	225	1.03
82	0.04	131	0.15	179	0.45	226	1.05
83	0.04	132	0.16	180	0.46	227	1.07
84	0.05	133	0.16	181	0.47	228	1.09
85	0.05	134	0.17	183	0.48	229	1.11
86	0.05	135	0.17	184	0.49	230	1.13
88	0.05	136	0.18	185	0.50	231	1.15
89	0.05	138	0.18	186	0.51	232	1.16
90	0.05	139	0.19	187	0.52	233	1.18
91	0.05	140	0.19	188	0.53	234	1.20
92	0.05	141	0.20	189	0.55	235	1.22
93	0.06	142	0.20	190	0.56	236	1.25
95	0.06	144	0.21	192	0.57	237	1.27
96	0.06	145	0.22	193	0.58	239	1.28
97	0.06	146	0.22	194	0.59	240	1.30
98	0.06	147	0.23	195	0.61	241	1.32
99	0.06	148	0.23	196	0.62	241	1.34
100	0.07	149	0.24	197	0.63	243	1.36
101	0.07	151	0.25	198	0.65	244	1.38
102	0.07	152	0.26	199	0.66	245	1.40
104	0.07	153	0.26	201	0.67	246	1.42
105	0.08	154	0.27	202	0.69	247	1.44
106	0.08	155	0.28	203	0.70	248	1.46
107	0.08	156	0.28	204	0.72	249	1.48
108	0.08	157	0.29	205	0.73		
109	0.09	159	0.30	206	0.75		

the air pressure. At lower temperatures, the uncertainty in the total pressure measurement dominates. At high temperature, the uncertainty in the estimation of air pressure dominates (because the air volumes are small).

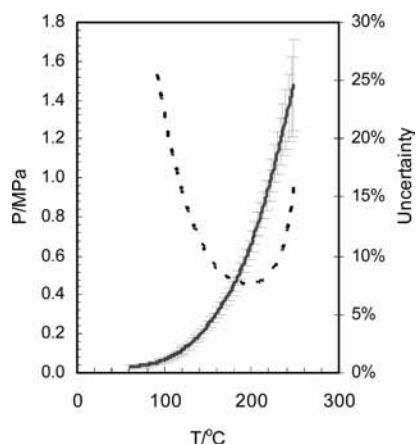


Figure 12. Predicted TMOS saturation pressure as a function of temperature from 3.0 mL volume data. Error bars shown represent an estimate of the absolute uncertainty. Percent relative uncertainty is shown as a function of temperature (dotted line).

Discussion

We have developed a relatively simple technique for measuring saturated liquid density and saturated pressure over a wide range of temperatures. The density and saturation pressure estimates for methanol obtained using this new technique show excellent agreement with those in the NIST database for methanol (Figures 5 and 6). Density and saturation pressure estimates for water agree with the NIST database over the lower half of the temperature range studied but are systematically high for temperatures above 190 °C (Figures 5 and 7). Subsequently, we applied the technique to the study of a compound, TMOS, for which literature values exist only over limited temperature ranges. We report here the first saturated liquid density and saturated pressure data (Figures 10 and 11, respectively) for TMOS over the temperature range (60 to 250) °C.

Estimation of the take-off temperature can be difficult. We applied a *somewhat* arbitrary, yet consistent, technique for determining take-off point, and this yielded good results. A comparison of Figures 3, 4, and 8 shows that methanol and TMOS each exhibit a more abrupt change in pressure than does water, which makes it easier to identify the take-off point for methanol or TMOS. This is consistent with the better match of the estimated densities for methanol than those for water to the higher-temperature NIST data.

We have used the ideal gas law to estimate the cell air pressure during processing and Dalton's Law to estimate saturation pressure. While these are applicable under the conditions tested, care should be taken if the technique is used under other conditions. The constant volume calculations of saturated liquid density neglect the volume of compressed air in the container. Based on the experimental results for water and air, we found that the relative error introduced by this assumption is insignificant compared to the other sources of uncertainty for the conditions used in this study. These effects are likely to become more important if smaller initial fill

volumes are used. Care must be used in the calculation of air pressure (eq 3). As the take-off point is approached, the model assumes that the volume of air goes to zero. The equation is only valid in the pre take-off region.

The technique uses a hydraulic hot press to provide a restraining force to seal the mold and to heat and cool the mold. An issue with the existing setup was that as the mold was compressed the gasket material deformed, changing the shape of the cell. As the pressure in the cell built up, it forced the gasket back out. Elimination of this problem, through the use of a different sealing mechanism, may improve the estimation of take-off. In an alternative approach to this technique, one could use a bolted system of fixed volume, heated with a film heater.

The high relative uncertainty values are only partially due to the technique. The estimate of the take-off temperature yields the highest uncertainty. We had scatter due to repeatability issues associated with the manual technique used to fill the mold. This could be improved with a redesigned mold. We could also have used more finely calibrated instrumentation; however, the values presented here are sufficient to prove the concept. Moreover, we note that the estimates with the highest relative uncertainty are in the temperature range (≤ 110 °C) for which previous values are available, and the values obtained with the new technique agree with those reported by Kato and Tanaka.¹

This paper describes a simple technique for measuring saturation pressure and saturated liquid densities. Data obtained for the well-characterized liquids methanol and water using this technique are comparable to those found in the literature. The technique is applied to the study of TMOS, resulting in the first such data for TMOS at temperatures from (60 to 250) °C.

Acknowledgment

We thank Dr. Philip Kosky for his input and advice.

Literature Cited

- (1) Kato, M.; Tanaka, H. Ebulliometric Measurement of Vapor–Liquid Equilibria for Four Binary Systems: Methanol + Silicon Tetramethoxide, Methanol + Silicon Tetraethoxide, Ethanol + Silicon Tetramethoxide, and Ethanol + Silicon Tetraethoxide. *J. Chem. Eng. Data* **1989**, *34*, 206–209.
- (2) Ivannikov, P. S.; Litvinenko, V. M.; Radchenko, I. V. Thermal Conductivity of Tetramethoxysilane, Tetraethoxysilane and Tetraethyl Tin. *J. Eng. Phys.* **1975**, *28*, 63–68.
- (3) Gauthier, B. M.; Bakrania, S. D.; Anderson, A. M.; Carroll, M. K. A Fast Supercritical Extraction Technique for Aerogel Fabrication. *J. Non-Cryst. Solids* **2004**, *350*, 238–243.
- (4) Lemmon, E. W.; McLinden, M. O.; Friend, D. G. Thermophysical Properties of Fluid Systems. In *NIST Chemistry WebBook, NIST Standard Reference Database Number 69*; Linstrom, P. J., Mallard, W. G., Eds.; National Institute of Standards and Technology: Gaithersburg, MD, 2005.

Received for review August 3, 2007. Accepted February 8, 2008. The authors acknowledge funding through the National Science Foundation (CTS-0216153 RUI/MRI and CHE-0514527 RUI) and the Union College Internal Education Fund. M.R.E. received a Union College Summer Research Fellowship.

JE700443D